**SUPPLEMENTAL INFORMATION FOR:**

# Paroxetine Is a Direct Inhibitor of G Protein-Coupled Receptor Kinase 2 and Increases Myocardial Contractility

David M. Thal[1], Kristoff T. Homan[1†], Jun Chen[2†], Emily K. Wu[1], Patricia M. Hinkle[3], Z. Maggie Huang[4], J. Kurt Chuprun[4], Jianliang Song[4], Erhe Gao[4], Joseph Y. Cheung[4], Larry Sklar[2], Walter J. Koch[4], and John J.G. Tesmer[1*]

[1]Life Sciences Institute and the Department of Pharmacology, University of Michigan, Ann Arbor, Michigan 48109

[2]Center for Molecular Discovery, University of New Mexico Health Sciences Center, Albuquerque, New Mexico 87131

[3]Department of Pharmacology and Physiology, University of Rochester Medical Center, Rochester, New York 14642

[4]Center for Translational Medicine, Temple University School of Medicine, Philadelphia, Pennsylvania 19140

[†]Equal contribution.
*Corresponding author: tesmerjj@umich.edu

## Supplementary Methods

**Materials and reagents.** RNA aptamers were synthesized by Integrated DNA Technologies. The original 51-nucleotide RNA aptamer (*1*) (C13.51) was truncated to create a smaller 28-nucleotide construct (C13.28) (*2*): 5′-GGCAGACCAUACGGGAGAGAAACUUGCC-3′. For direct binding and competition assays, C13.28 was fluorescently labeled on the 3′ end with 6-carboxyfluorescein (C13.28-FAM). [$\gamma$-$^{32}$P]ATP was purchased from MP Biomedicals. Dark adapted bovine retinas were purchased from W.L. Lawson Company. Paroxetine ((3S-trans)-3-[(1,3-benzodioxol-5-yloxy)methyl]-4-(4-fluorophenyl)piperidine hydrochloride), defluoro paroxetine (3-[(1,3-benzodioxol-5-yloxy)methyl]-4-phenyl-piperidine HCl), desmethylene paroxetine (4-[[(3S,4R)-4-(4-fluorophenyl)-3-piperidinyl]-1,2-benzenediol HCl), and fluoxetine (N-methyl-γ-[4-(trifluoromethyl)phenoxy]benzenepropanamine HCl) were purchased from Toronto Research Chemicals. Bovine brain tubulin (>99% pure) was purchased from Cytoskeleton, Inc. 1-Anilinonaphthalene-8-sulfonic acid (ANS) was purchased from Sigma-Aldrich.

**Flow cytometry bead binding assay.** Human GRK2 was biotinylated (bGRK2) using biotin N-hydroxysuccinimide ester (Sigma) and conjugated to streptavidin coated beads (Spherotech). bGRK2–labeled beads were resuspended in GRK2 assay buffer (20 mM HEPES pH 7.0, 10–50 mM NaCl, 5 mM $MgCl_2$, 1 mM CHAPS, 0.1% lubrol, and 2 mM DTT). For equilibrium binding, GRK2 labeled beads were added to serial dilutions of C13.28-FAM and allowed to equilibrate

for 1 hr at room temperature before being processed on an Accuri C6 flow cytometer equipped with a HyperCyt Autosampler. Binding data was fit using nonlinear regression, accounting for non-specific binding, using GraphPad Prism v5.0d. Competition binding assays were performed by adding 5 μl of GRK2 labeled beads to 10 μl of serially diluted competitors and allowed to incubate at room temperature for 15–30 min before adding 5 μl of 8.0 nM (2.0 nM final) C13.28-FAM. Plates were allowed to equilibrate for 1 hr at room temperature before being processed. Data was normalized to positive (blank beads) and negative (no inhibitor) controls and fit to a four-parameter dose-response model using nonlinear regression with GraphPad Prism.

**Prestwick Chemical Library screen.** Peak 1 and Peak 6 beads from Spherotech streptavidin blue array particles were used to adapt the bead binding assay into a duplex format. Peak 1 and Peak 6 beads were conjugated with bGRK2 and biotinylated C13.28-FAM (bC13.28-FAM; as a counter screen), respectively, and mixed. A total of volume of 10 μl reaction was added to wells in the following sequence: 4 μL GRK2 assay buffer; 100 nl of 1 mM compound; 3 μl mixed beads followed by incubation at room temperature for 15 min; and 3 μl C13.28-FAM. Plates were then incubated upside-down at room temperature for 1 hr and analyzed by flow cytometry using the HyperCyt® platform at the University of New Mexico Center for Molecular Discovery. Flow cytometric light scatter and fluorescence emission at 530 ± 20 nm (FL1) and 665 ± 10 nm (FL8) were collected. FL8 fluorescence was used to distinguish Peak 1 and Peak 6 beads.

Median fluorescence intensity (MFI) of FL1 channel was used to calculate assay response. Z´ was defined by replicate control wells containing 1% DMSO vehicle control or 50 × unlabeled C13.28. Hits were defined for the assay based on their ability to decrease the MFI of FL1 channel on Peak 1 beads below 3 σ from the DMSO controls, but to not decrease the MFI of FL1 channel on Peak 6 beads lower than 60% of the DMSO control (Supplementary Figure 1).

**Thermostability Measurements.** The $T_m$ of GRK1, GRK2, and GRK5 in the presence or absence of 200 μM ligand were determined by measuring the fluorescence change of ANS as it binds to unfolded protein (*3*). Purified protein (0.2 mg $ml^{-1}$) and ligand were incubated with 100 μM ANS in a total volume of 5 μl, in triplicate, in ABgene 384-well PCR microtiter plates (Thermo-Fisher). Fluorescence was measured over an increasing temperature range in 1 ºC intervals using a Thermofluor 384-well plate reader (Johnson & Johnson). Melting curves were analyzed by fitting to a Boltzmann model using Thermofluor Acquire 3.0 software.

**Phosphorylation data analysis.** Data was fit using nonlinear regression using a four-parameter fit as described in equation 1:

$$Y = Bottom + \frac{(Top - Bottom)}{\left(1 + 10^{(logIC_{50} - X) \times n_H)}\right)} \qquad (1)$$

where *X* is the log [inhibitor], *Y* is the response, $n_H$ is the Hill slope, and *Top* and *Bottom* are the plateaus of the response. Significance between reactions was assessed using unpaired t-tests in GraphPad Prism v5.0d.

**GRK2 mediated phosphorylation of TRH receptors.** HEK293 cells stably expressing HA-tagged rat TRH receptors were used to measure receptor phosphorylation. Cells were seeded in 24-well dishes coated with poly-D-lysine, grown for two days and equilibrated in Hank's balanced salt solution at room temperature for experiments. Cells were pre-incubated with inhibitors for 45 min and then stimulated with TRH for 15 s. Reactions were stopped with 2 ml $well^{-1}$ of 1:1 (v/v) methanol:acetone at room temperature, which fixed the cells. Receptor phosphorylation was measured in an ELISA protocol as previously described (*4*) using affinity-purified rabbit antibody Ab6959 at 1:1000. This antibody recognizes TRH receptors phosphorylated at Ser and Thr residues between amino acids 355 and 365 in the cytoplasmic tail. Data was fit using non-linear regression with a fixed slope.

**Crystallization and structure determination.** Human GRK2 (1.9 mg) and bovine $G\beta_1\gamma_2$C68S (1.5 mg) were gel filtered into 20 mM HEPES pH 8.0, 50 mM NaCl, 5 mM $MgCl_2$, and 2 mM DTT, and then mixed together and concentrated to 8 mg $ml^{-1}$. Paroxetine was dissolved in the gel filtration buffer at a concentration of 15 mM and added to GRK2–$G\beta_1\gamma_2$C68S to a final concentration of 1 mM. GRK2·paroxetine–$G\beta_1\gamma_2$C68S was crystallized by the hanging drop method at 4 °C using a 1:1 mixture in a well solution containing 100 mM MES pH 5.8, 200 mM NaCl, and 8% (w/v) PEG3350. Crystals were harvested in a cryoprotectant solution containing 20 mM HEPES pH 8.0, 100 mM MES pH 5.8, 250 mM NaCl,

5 mM $MgCl_2$, 2 mM DTT, 9% (w/v) PEG3350, 25% (v/v) ethylene glycol and 1 mM paroxetine. Diffraction data were collected at the Advanced Photon Source at LS-CAT beam line 21-ID-F. Diffraction intensities were observed out to 2.07 Å spacings and was anisotropic, and therefore ellipsoidal truncation (2.07 Å in the direction of *hk0*, and 2.5 Å along *–hk0* and *k*) was performed on unmerged reflections before scaling with SCALEPACK (*5*), as previously described (*6*). The phases for the structure were solved by molecular replacement with PHASER (*7*). The structure of GRK2–$G\beta_1\gamma_2$ (PDB: 1OMW) was used to generate two search models: 1) the large lobe of the kinase domain and 2) the remainder of the structure. The initial coordinates and stereochemical parameters for paroxetine were derived from the published crystal structure (*8*). Models for the GRK2·paroxetine–$G\beta_1\gamma_2$C68S structure were generated with COOT (*9*) and refined using TLS (*10*) and restrained refinement (*11*) in REFMAC5. MolProbity (*12*) and PROCHECK (*13*) were used for structure validation. The final model includes residues 30–484, 494–568, and 576–668 of GRK2, 2–340 of $G\beta_1$, and 8–64 of $G\gamma_2$. Crystallographic and refinement statistics are given in Supplementary Table 2. The atomic model and structure factors are deposited with the Protein Data Bank as entry 3V5W.

## Supplementary Figures

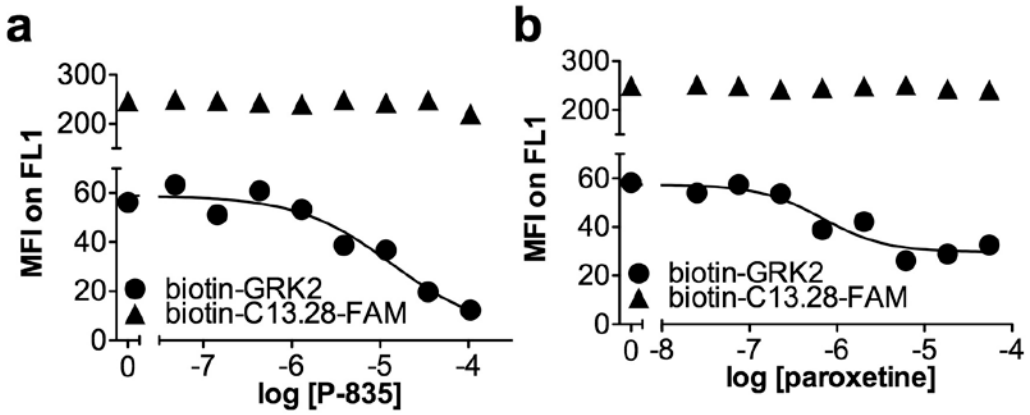


**Supplementary Figure 1. Flow cytometry bead binding assay counter-screen using bC13.28-FAM.** Original dose-response titrations of (**a**) P-835 and (**b**) paroxetine (P851) against peak 1 (circles) and 6 (triangles) blue array particles conjugated to bGRK2 and bC13.28-FAM, respectively. Neither compound significantly diminished median fluorescence intensity (MFI) of the peak 6 beads on the FL1 channel (530 ± 20 nm) suggesting that the compounds do not interfere with the fluorescence properties of C13.28-FAM.

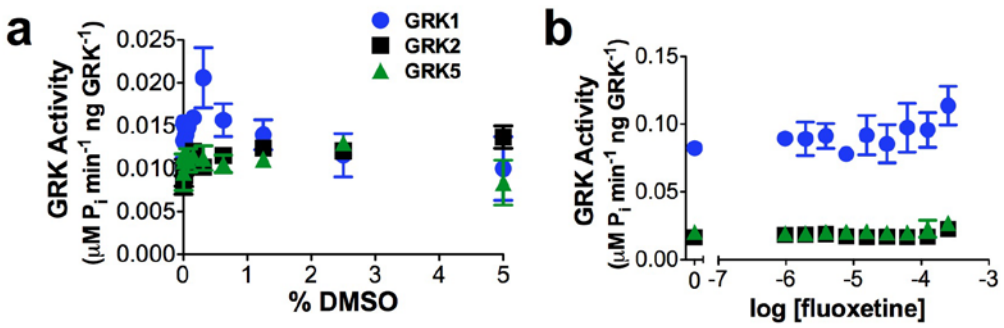


**Supplementary Figure 2. DMSO (a) and the SSRI fluoxetine (b) do not inhibit phosphorylation of ROS by GRK1, 2 and 5.**

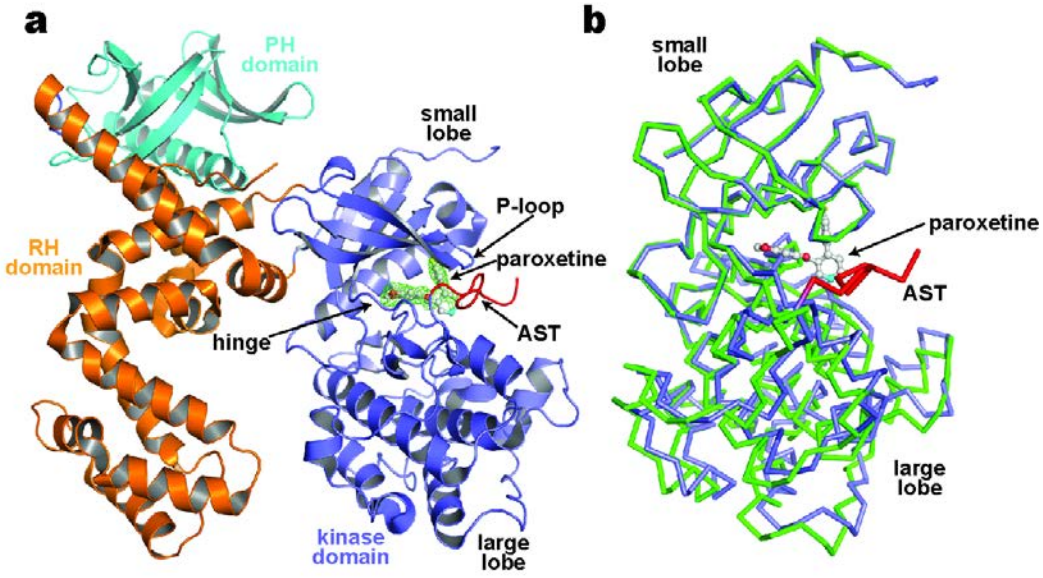


**Supplementary Figure 3. Structural features of the GRK2·paroxetine–Gβγ complex.** (**a**) Paroxetine binds in the ATP binding site, adjacent to a section of the active site tether (AST). Corresponding electron density from an m|$F_o$|–D|$F_c$| omit map contoured at 3 σ is shown as a green cage. The overall structure of the GRK2·paroxetine complex is shown with the kinase domain colored slate, the AST region red, the regulator of G protein signaling homology (RH) domain orange, and the pleckstrin homology (PH) domain cyan. Gβγ, which binds to the PH domain, is omitted for clarity. (**b**) The GRK2 kinase domain in complex with paroxetine adopts a conformation distinct from those of previously published GRK2 structures, as evidenced by ordering of the AST and the change in orientation of the large lobe relative to the small lobe. The Cα traces of the kinase domains from the GRK2·paroxetine (this paper) and GRK2·103A (PDB: 3PVW; (*14*)) complexes are shown in slate and green, respectively, and were superimposed using their small lobes.

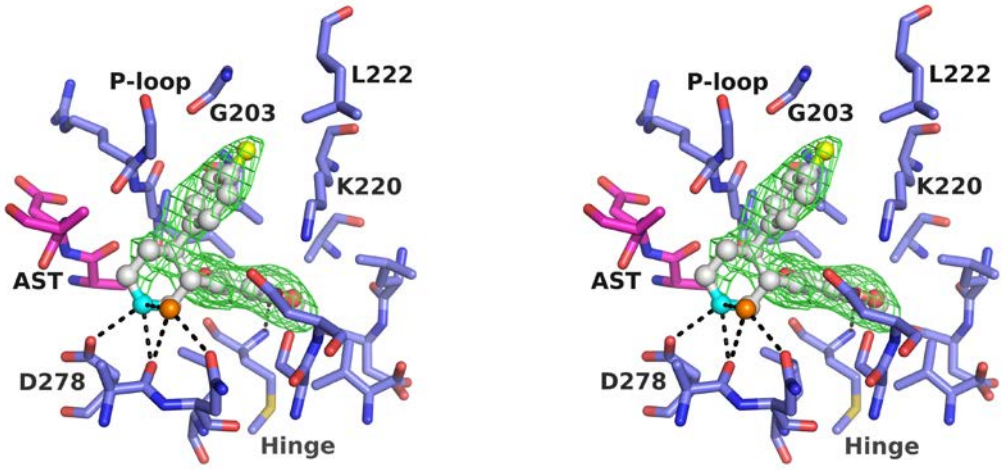


**Supplementary Figure 4. Stereo-view of residues interacting with paroxetine.** Electron density for paroxetine is shown as a green cage from an m|$F_o$|–D|$F_c$| omit map contoured at 3 σ. Residues from GRK2 are shown as sticks with carbons colored slate (magenta for the AST), nitrogens blue, oxygens red, and water orange. Paroxetine is shown as a ball-and-stick model with carbons colored white, nitrogens cyan, oxygens red, and fluorine yellow. Potential hydrogen bonds are shown as dotted lines.

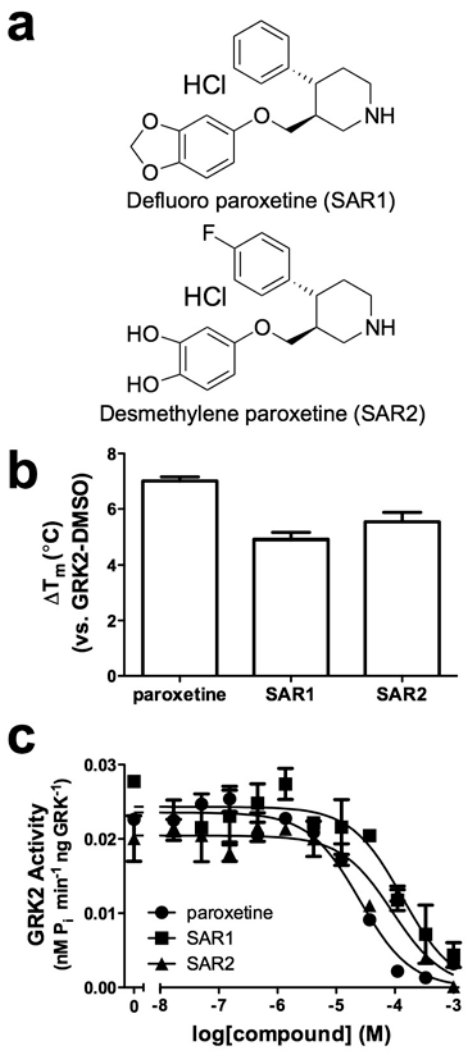


**Supplementary Figure 5. Derivatives of paroxetine exhibit predictably less potency against GRK2.** (**a**) Structures of defluoro paroxetine (SAR1) and desmethylene paroxetine (SAR2) (*cf.* Figure 2e). (**b**) Both derivatives thermostabilize GRK2 to a lesser extent than paroxetine ($P < 0.0001$ and $P = 0.0011$ for SAR1 and SAR2, respectively). Data shown are mean values ± SEM ($n=3$), performed in triplicate. (**c**) Defluoro and desmethylene paroxetine are significantly less potent inhibitors of GRK2. Data shown is representative of three or more experiments performed in duplicate (see Supplementary Table 3). $P = 0.01$ and $P = 0.0033$ for SAR1 and SAR2 relative to paroxetine, respectively.

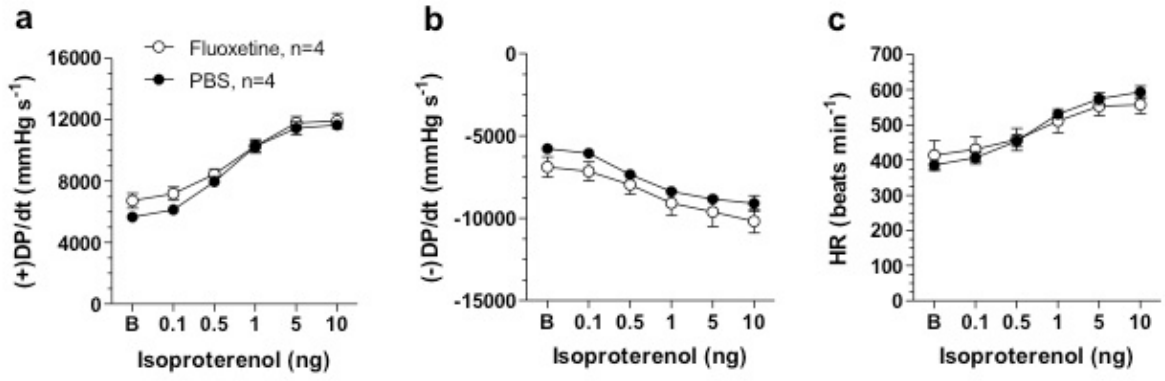


**Supplementary Figure 6. Fluoxetine has no significant effect on *in vivo* cardiac contractility.** Mice were treated as in Figure 6 with a 1 hr pre-treatment of PBS (*n*=4) or fluoxetine (10 mg $kg^{-1}$, *n*=4) and then *in vivo* hemodynamics in response to increasing doses of isoproterenol were administered. (**a**) Basal and isoproterenol dose-response for LV +dP/dt (mean ± SEM). (**b**) Basal and isoproterenol dose-response for LV –dP/dt (mean ± SEM). (**c**) Basal and isoproterenol dose-response for heart rate (HR) (mean ± SEM).

**Supplementary Table 1. HTS screening data**

| Category | Parameter | Description |
|---|---|---|
| Assay | Type of assay | Flow Cytometry Protein Interaction |
| | Target | G Protein-Coupled Receptor Kinase 2 |
| | Primary measurement | Median fluorescence intensity on FL1 channel |
| | Key reagents | C13.28-FAM aptamer from www.idtdna.com |
| | Assay protocol | See Supplementary Methods |
| Library | Library size | 1200 compounds |
| | Library composition | Mostly FDA approved drugs |
| | Source | Prestwick Chemical http://www.prestwickchemical.com/ |
| Screen | Format | 384-well plates |
| | Concentration(s) tested | 10 μM compound, 1% DMSO final |
| | Plate controls | 1% DMSO & 50X unlabeled C13.28 |
| | Detection instrument and software | HyperCyt® platform |
| | Assay validation/QC | Z´ score |
| | Correction factors | N/A |
| | Normalization | N/A |
| | Additional comments | Screened at UNM Center for Molecular Discovery |
| Post-HTS analysis | Hit criteria | 3 σ below DMSO control |
| | Hit rate | 0.2% (2 out of 1200 compounds) |
| | Additional assay(s) | Counter-screen using biotinylated C.13.28-FAM with 60% DMSO control cut-off, retest in flow cytometry bead binding assay with dose-response titrations |
| | Confirmation of hit purity and structure | Paroxetine was purchased from both Prestwick and Toronto Research Group |

**Supplementary Table 2. Crystallographic data and refinement statistics**

| | |
|---|---|
| X-ray source: | APS 21-ID-F |
| Wavelength (Å) | 0.9786 |
| $D_{min}$ (Å) | 25–2.07 (2.11–2.07) |
| Space group | *C*2 |
| Cell constants | *a* = 195.0 Å |
| | *b* = 71.0 Å |
| | *c* = 111.2 Å |
| | β = 110.4° |
| Unique reflections | 55,040 (12) |
| Average multiplicity | 2.6 (1.2) |
| $R_{sym}$ (%) | 7.7 (59.7) |
| Completeness (%) | 61.8 (0.3) |
| $\langle I \rangle / \langle \sigma_I \rangle$ | 16.8 (1.5) |
| Refinement resolution (Å) | 24.5–2.07 (2.12–2.07) |
| Total reflections used | 52,208 (85) |
| Non-protein atoms | 327 |
| RMSD bond lengths (Å) | 0.008 |
| RMSD bond angles (°) | 1.2 |
| Est. coordinate error (Å) | 0.15 |
| Ramachandran plot | |
| most favored, disallowed (%) | 91.1, 0.0 |
| $R_{work}$ | 19.3 (30.7) |
| $R_{free}$ | 24.7 (32.0) |
| Protein atoms | 8,255 |
| Water molecules | 296 |
| Paroxetine atoms | 24 |
| Average B-factor (Å$^2$) | |
| GRK2 | 60 |
| Paroxetine | 57 |
| PDB Entry | 3V5W |

**Supplementary Table 3. Summary of structure-activity relationship data**

| | paroxetine | | defluoro paroxetine | | | desmethylene paroxetine | | |
|---|---|---|---|---|---|---|---|---|
| | $pIC_{50}$ | *n* | $pIC_{50}$ | *n* | fold | $pIC_{50}$ | *n* | fold |
| ROS | 4.4 ± 0.1 | *6* | 3.5 ± 0.6 | *4* | 8 | 4.2 ± 0.4 | *6* | 2 |
| SepiaRho | 4.8 ± 0.06 | *3* | 4.0 ± 0.05 | *5* | 6 | 4.1 ± 0.07 | *3* | 5 |

Values represent the calculated $IC_{50}$ ± SEM of at least 3 experiments, performed in duplicate for GRK2-mediated phosphorylation of either bovine rhodopsin (ROS) or *Sepia* rhodopsin (SepiaRho) with 100 μM ATP. Fold changes for the defluoro and desmethylene paroxetine compounds are calculated versus paroxetine (see **Supplementary Figure 5c**): P = 0.0012 and P = 0.40 for the ROS assays, and P = 0.01 and P = 0.003 for the Sepia rhodopsin assays, respectively.

**Supplementary Table 4. Myocyte contractility in response to fluoxetine**

| | Control | Fluoxetine | Significance |
|---|---|---|---|
| **Baseline before isoproterenol** | | | |
| Max. contraction amplitude (% cell length) | 4.6 ± 0.6 | 4.8 ± 0.4 | NS |
| **After isoproterenol** | | | |
| Max. contraction amplitude (% cell length) | 13.2 ± 1.3 | 12.0 ± 1.7 | NS |
| % increase in contraction amplitude | 191.1 ± 11.8 | 154.5 ± 31.8 | NS |

Values represent the mean ± SEM of *n*=4 experiments. NS = no significance.

## Supplementary References


1. Mayer, G., Wulffen, B., Huber, C., Brockmann, J., Flicke, B., Neumann, L., Hafenbradl, D., Klebl, B. M., Lohse, M. J., Krasel, C., and Blind, M. (2008) An RNA molecule that specifically inhibits G-protein-coupled receptor kinase 2 in vitro, *RNA 14*, 524-534.
2. Tesmer, V. M., Lennarz, S., Mayer, G., and Tesner, J. J. G. (2012) Molecular mechanism for inhibition of G protein- coupled receptor kinase 2 by a selective RNA aptamer, *Structure*, in press.
3. Mezzasalma, T. M., Kranz, J. K., Chan, W., Struble, G. T., Schalk-Hihi, C., Deckman, I. C., Springer, B. A., and Todd, M. J. (2007) Enhancing recombinant protein quality and yield by protein stability profiling, *J. Biomol. Screen. 12*, 418-428.
4. Jones, B. W., Song, G. J., Greuber, E. K., and Hinkle, P. M. (2007) Phosphorylation of the endogenous thyrotropin-releasing hormone receptor in pituitary GH3 cells and pituitary tissue revealed by phosphosite-specific antibodies., *J. Biol. Chem. 282*, 12893-12906.
5. Otwinoski, Z., and Minor, W. (1997) Processing of X-ray diffraction data collected in oscillation mode, *Methods Enzymology 276*, 307-326.
6. Lodowski, D. T., Pitcher, J. A., Capel, W. D., Lefkowitz, R. J., and Tesmer, J. J. G. (2003) Keeping G proteins at bay: a complex between G protein-coupled receptor kinase 2 and Gβγ., *Science 300*, 1256-1262.
7. McCoy, A. J., Grosse-Kunstleve, R. W., Adams, P. D., Winn, M. D., Storoni, L. C., and Read, R. J. (2007) Phaser crystallographic software., *J. Appl. Crystallogr. 40*, 658-674.
8. Ibers, J. A. (1999) Paroxetine hydrochloride hemihydrate, *Acta Crystallogr. Sect. C: Cryst. Struct. Commun. 55*, 432-434.
9. Emsley, P., and Cowtan, K. (2004) Coot: model-building tools for molecular graphics., *Acta Crystallogr. Sect. D. Biol. Crystallogr. 60*, 2126-2132.
10. Winn, M. D., Isupov, M. N., and Murshudov, G. N. (2001) Use of TLS parameters to model anisotropic displacements in macromolecular refinement, *Acta Crystallogr. Sect. D. Biol. Crystallogr. 57*, 122-133.
11. Murshudov, G. N., Vagin, A. A., and Dodson, E. J. (1997) Refinement of macromolecular structures by the maximum-likelihood method, *Acta Crystallogr. Sect. D. Biol. Crystallogr. 53*, 240-255.
12. Chen, V. B., Arendall, W. B., Headd, J. J., Keedy, D. A., Immormino, R. M., Kapral, G. J., Murray, L. W., Richardson, J. S., and Richardson, D. C. (2010) MolProbity: all-atom structure validation for macromolecular crystallography., *Acta Crystallogr. Sect. D. Biol. Crystallogr. 66*, 12-21.
13. Laskowski, R. A., MacArthur, M. W., Moss, D. S., and Thornton, J. M. (1993) PROCHECK: a program to check the stereochemical quality of protein structures, *J. Appl. Crystallogr. 26*, 283-291.
14. Thal, D. M., Yeow, R. Y., Schoenau, C., Huber, J., and Tesmer, J. J. G. (2011) Molecular mechanism of selectivity among G protein-coupled receptor kinase 2 inhibitors., *Mol. Pharmacol. 80*, 294-303.